



NURBS-augmented finite element method for stability analysis of arbitrary thin plates

Biraja Prasad Mishra¹ · Manoranjan Barik¹

Received: 16 February 2018 / Accepted: 16 March 2018 / Published online: 21 March 2018
© Springer-Verlag London Ltd., part of Springer Nature 2018

Abstract

In the analysis of a plate, the geometry plays a very important role. The non-uniform rational B-spline (NURBS) basis functions are employed for the representation of the geometry and field variables in the isogeometric analysis. These basis functions are able to represent the geometry accurately. They are non-interpolating in nature, and hence do not satisfy the Kronecker-Delta property. Hence, it becomes difficult to enforce the essential boundary conditions at the control variables. A new method called NURBS-augmented finite element method (NAFEM) was proposed (Mishra and Barik, *Comput Struct*, <https://doi.org/10.1016/j.compstruc.2017.10.011>, 2017) and arbitrary shaped plates were successfully dealt for bending analysis. In the NAFEM, the authors adopted the finite element basis functions for the field variables as they satisfy the Kronecker-Delta property so that the boundary conditions were enforced with ease and the NURBS basis functions were employed for the geometry, thereby representing the shape of the plate accurately. In the present work, the same is extended for stability analysis of plates having different geometries and boundary conditions and the results are found to be in excellent agreement with the existing ones. Some new shapes have also been considered, and the new results are presented.

Keywords NURBS-augmented finite element method (NAFEM) · Isogeometric analysis (IGA) · Non-uniform rational B-spline (NURBS) · Finite element analysis (FEA) · Stability analysis · Arbitrary thin plates

1 Introduction

The finite element analysis is a numerical technique to solve various problems in the field of engineering such as structural analysis, heat transfer, fluid flow, etc. In the structural analysis, the geometry plays a vital role which can be achieved with a great accuracy with the help of Computer-aided Design (CAD). The FEA programs developed long before CAD were susceptible to inaccuracies. In order to vanquish this impediment Hughes et al. [7] proposed a concept called isogeometric analysis (IGA) which was successful in integrating the CAD and FEA resulting in representing the geometry accurately; where the non-uniform rational B-splines (NURBS) basis functions were engaged in representing the geometry and the field variables. However, the

NURBS basis functions are non-interpolating in nature and do not satisfy the Kronecker-Delta which result in the difficulty in enforcing the essential boundary condition [6, 10] and needed special treatment. A number of methods have been developed to impose the essential boundary conditions. Some of the most popular methods are Lagrange multiplier method [4], penalty method [24] and Nitsche method [6].

The buckling analysis of clamped elliptical plates was first carried out by Woinowsky-Krieger [22] subjected to uniform compression. A semi-analytical semi-numerical method of solution was presented by Zhou et al. [23] for the stability analysis of simply supported sector plates. The stability analysis of rectangular Mindlin plates having with different boundary conditions have been studied by Liew et al. [8] by using the Levy-type solution method.

Thai et al. [15] presented a new inverse tangent shear deformation theory (ITSDT), layerwise deformation theory [16], higher order shear deformation theory [17] for the bending, free vibration and stability analysis of laminated composite and sandwich plates of arbitrary shapes using isogeometric analysis. The behaviour of laminated composite Reissner–Mindlin plates of various shapes using NURBS

✉ Manoranjan Barik
manoranjanbarik@yahoo.co.in

Biraja Prasad Mishra
birajanit@gmail.com

¹ Department of Civil Engineering, National Institute of Technology, Rourkela, Odisha 769008, India

based isogeometric analysis under bending, vibration and stability can be found in [18] and [3].

The isogeometric analysis has been used for studying the static, vibration and buckling behaviour of isotropic and laminated composite structures [13, 14, 20, 21], etc. Mishra and Barik [9] coined a new term NURBS-Augmented Finite Element Method (NAFEM) similar to the one used in [12] but with a difference. In this NAFEM the geometry of the plate is represented by NURBS basis functions, whereas the displacement functions for all the elements which include the internal as well as the boundary elements are represented by the classical finite elements.

It is apparent that though IGA is efficient in integrating CAD and FEA, its inherent problem with the imposition of boundary condition makes it a poor choice for the finite element analysis. In the present work, the boundary condition imposition problem is alleviated by replacing the NURBS with classical finite element basis function to represent the field variables.

2 Proposed analysis

2.1 Stability analysis

The equation of equilibrium for the stability analysis is given by

$$[K]\{\delta\} - \lambda[K_G]\{\delta\} = \{0\}, \tag{1}$$

where $[K]$ and $[K_G]$ are the global elastic stiffness and geometric stiffness matrices, respectively, $\{\delta\}$ is the displacement vector in the global coordinate system.

2.2 NURBS basis function

Given a knot vector $S = \{s_1, s_2, s_3, \dots, s_{n+p+1}\}$, the associated set of B-spline basis functions $\{N_{i,p}\}_{i=1}^n$ are defined recursively

by the Cox–de Boor formula, starting with the zeroth order basis function ($p = 0$) as

$$N_{i,0} = \begin{cases} 1 & \text{if } s_i \leq s \leq s_{i+1} \\ 0 & \text{otherwise} \end{cases} \tag{2}$$

and for a polynomial order $p \geq 1$

$$N_{i,p}(s) = \frac{s - s_i}{s_{i+p} - s_i} N_{i,p-1}(s) + \frac{s_{i+p+1} - s}{s_{i+p+1} - s_{i+1}} N_{i+1,p-1}(s), \tag{3}$$

where n is the number of basis functions and p is the order of the basis functions. The fractions of the form $0 / 0$ are defined as zero.

2.3 Mapping of the plate

The use of NURBS basis functions for the representation of geometry introduces the concept of parametric space which is absent in the conventional finite element formulation [9, 11]. The consequence of this additional space is that an additional mapping is performed to operate in the parent element coordinates. First, the parent space is mapped to the parametric space and then to the physical space (Fig. 1).

The mapping from parametric to physical space is given by

$$[X] = \sum_{i=1}^n \sum_{j=1}^m P_{i,j} R_{i,j}^{p,q}(s, t), \tag{4}$$

where $P_{i,j}$ are the control points and $R_{i,j}^{p,q}(s, t)$ is the bivariate NURBS basis function defined as

$$R_{i,j}^{p,q}(s, t) = \frac{N_i(s)M_j(t)w_{i,j}}{\sum_{i=1}^n \sum_{j=1}^m N_i(s)M_j(t)w_{i,j}} \tag{5}$$

$N_i(s)$ and $M_j(t)$ are the univariate B-spline basis functions of order p and q corresponding to the knot vectors in the respective directions and $\{w_{i,j}\}_{i=1,j=1}^{n,m}$, where $w_{i,j} > 0$ are the

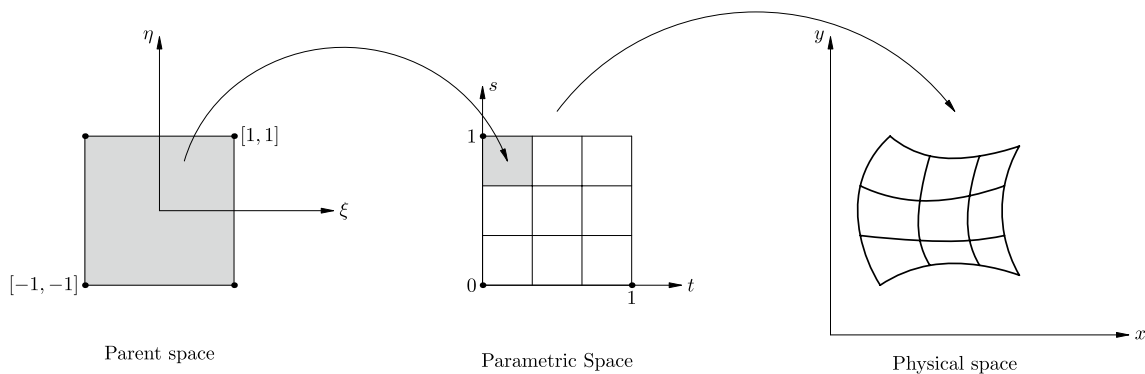


Fig. 1 Mapping parent to physical space through parametric space

set of NURBS weights. The mapping from parent to parametric space is given by [9, 11]

$$s(\xi) = \frac{(s_{i+1} - s_i)\xi + (s_{i+1} - s_i)}{2}, \quad t(\eta) = \frac{(t_{i+1} - t_i)\eta + (t_{i+1} - t_i)}{2} \tag{6}$$

The geometries in the physical space may also be divided into simple patches and then those patches are mapped to the parent space through the parametric space. As a typical example the physical space defined by the coordinates ACDB is divided into two patches namely ACFE and EFDB as shown in Fig. 2. The parent space is then mapped to two patches in the physical space through the parametric space and the procedure is followed as before to compute the stiffness matrix of each patch. The stiffness matrices of all the patches are assembled to form the global stiffness matrix of the whole plate. Thus the analysis of the plates can be made simpler by subdividing them into more amenable patches which can be dealt with ease [9].

2.4 Displacement interpolation function

For the proposed element, the four-noded rectangular non-conforming ACM plate bending element with 12° of freedom is taken as the basic element. As the element is in $\xi - \eta$ plane the shape functions and the nodal parameters for the displacements and slopes are expressed in terms of the coordinates

$\xi - \eta$ unlike the $x - y$ coordinates of the parent ACM element [2]. Thus the displacement function can be written as [9]:

$$w = [N_w] \{ \delta \}, \tag{7}$$

where

$$[N_w] = [N_w^1 N_{\theta_\xi}^1 N_{\theta_\eta}^1 \dots N_w^4 N_{\theta_\xi}^4 N_{\theta_\eta}^4], \tag{8}$$

$$\{ \delta \} = \left[w_1 \left(\frac{\partial w}{\partial \xi} \right)_1 \left(\frac{\partial w}{\partial \eta} \right)_1 \dots w_4 \left(\frac{\partial w}{\partial \xi} \right)_4 \left(\frac{\partial w}{\partial \eta} \right)_4 \right]^T. \tag{9}$$

The shape functions for the displacement field for the j th node are given as:

$$[N_w^j N_{\theta_\xi}^j N_{\theta_\eta}^j] = \frac{1}{8} \begin{bmatrix} (s_0 + 1)(t_0 + 1)(2 + s_0 + t_0 - \xi^2 - \eta^2) \\ s_j(s_0 + 1)^2(s_0 - 1)(t_0 + 1) \\ t_j(s_0 + 1)(t_0 + 1)^2(t_0 - 1) \end{bmatrix}, \tag{10}$$

where $s_0 = \xi s_j$ and $t_0 = \eta t_j$.

2.5 Strain–displacement matrix

The displacement functions of the plate element is expressed in terms of the local coordinate system $\xi - \eta$, whereas strains are in terms of the derivatives of the

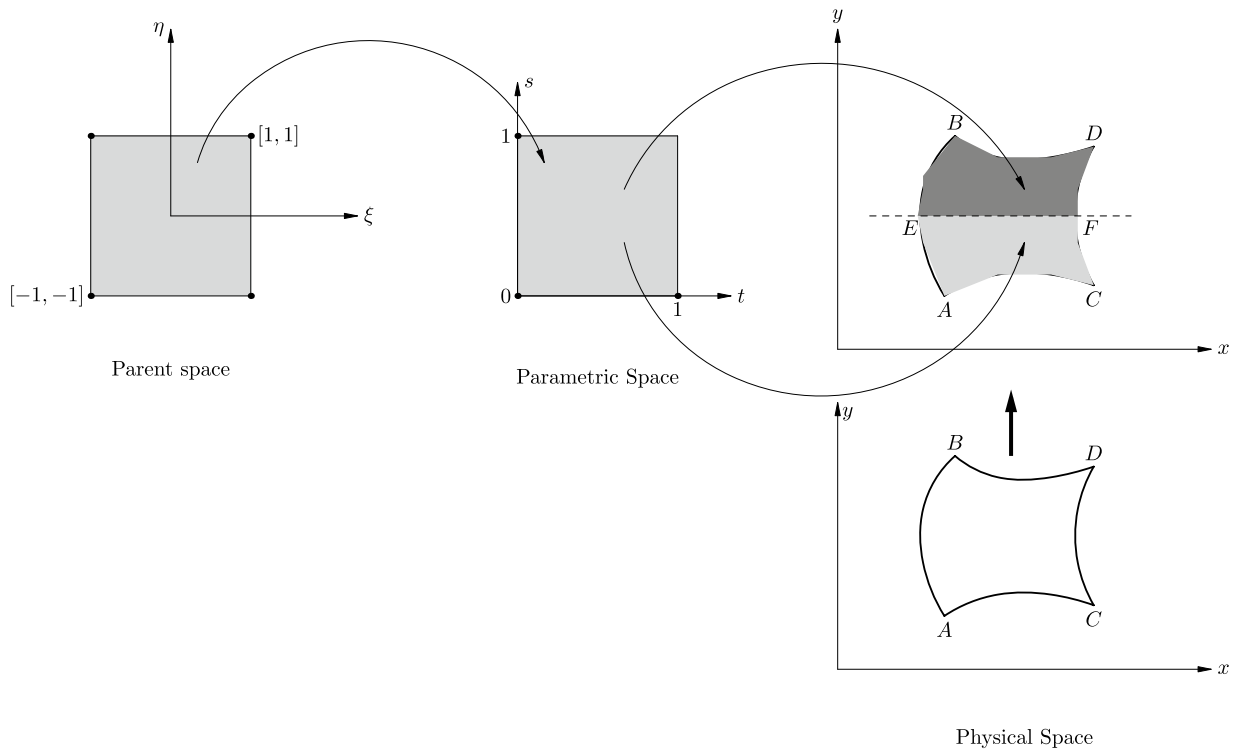


Fig. 2 Mapping parent to the different patches in physical space through parametric space

displacements with respect to $x - y$ coordinates. Hence before establishing the relationship between the strain and displacement, the first- and second-order derivatives of the displacements w with respect to the $x - y$ coordinates are expressed in terms of those of local coordinates $(\xi - \eta)$ using the chain rule of differentiation and are obtained as [9]:

$$\begin{Bmatrix} \frac{\partial w}{\partial \xi} \\ \frac{\partial w}{\partial \eta} \end{Bmatrix} = \begin{bmatrix} \frac{\partial s}{\partial \xi} & \frac{\partial t}{\partial \xi} \\ \frac{\partial s}{\partial \eta} & \frac{\partial t}{\partial \eta} \end{bmatrix} \begin{Bmatrix} \frac{\partial w}{\partial s} \\ \frac{\partial w}{\partial t} \end{Bmatrix} = [J1] \begin{Bmatrix} \frac{\partial w}{\partial s} \\ \frac{\partial w}{\partial t} \end{Bmatrix} \quad (11)$$

Differentiating Eq. (11) with respect to ξ and η

$$\begin{Bmatrix} \frac{\partial^2 w}{\partial \xi^2} \\ \frac{\partial^2 w}{\partial \eta^2} \\ \frac{\partial^2 w}{\partial \xi \partial \eta} \end{Bmatrix} = \begin{bmatrix} \frac{\partial^2 s}{\partial \xi^2} & \frac{\partial^2 t}{\partial \xi^2} \\ \frac{\partial^2 s}{\partial \eta^2} & \frac{\partial^2 t}{\partial \eta^2} \\ \frac{\partial^2 s}{\partial \xi \partial \eta} & \frac{\partial^2 t}{\partial \xi \partial \eta} \end{bmatrix} \begin{Bmatrix} \frac{\partial w}{\partial s} \\ \frac{\partial w}{\partial t} \end{Bmatrix} + \begin{bmatrix} \left(\frac{\partial s}{\partial \xi}\right)^2 & \left(\frac{\partial t}{\partial \xi}\right)^2 & 2\frac{\partial s}{\partial \xi} \frac{\partial t}{\partial \xi} \\ \left(\frac{\partial s}{\partial \eta}\right)^2 & \left(\frac{\partial t}{\partial \eta}\right)^2 & 2\frac{\partial s}{\partial \eta} \frac{\partial t}{\partial \eta} \\ \left(\frac{\partial s}{\partial \xi} \frac{\partial s}{\partial \eta}\right) & \left(\frac{\partial t}{\partial \xi} \frac{\partial t}{\partial \eta}\right) & \left(\frac{\partial s}{\partial \xi} \frac{\partial t}{\partial \eta} + \frac{\partial s}{\partial \eta} \frac{\partial t}{\partial \xi}\right) \end{bmatrix} \begin{Bmatrix} \frac{\partial^2 w}{\partial s^2} \\ \frac{\partial^2 w}{\partial t^2} \\ \frac{\partial^2 w}{\partial s \partial t} \end{Bmatrix} = [J2][J1]^{-1} \begin{Bmatrix} \frac{\partial w}{\partial s} \\ \frac{\partial w}{\partial t} \end{Bmatrix} + [J3] \begin{Bmatrix} \frac{\partial^2 w}{\partial s^2} \\ \frac{\partial^2 w}{\partial t^2} \\ \frac{\partial^2 w}{\partial s \partial t} \end{Bmatrix} \quad (12)$$

Also we have,

$$\begin{Bmatrix} \frac{\partial w}{\partial s} \\ \frac{\partial w}{\partial t} \end{Bmatrix} = \begin{bmatrix} \frac{\partial x}{\partial s} & \frac{\partial y}{\partial s} \\ \frac{\partial x}{\partial t} & \frac{\partial y}{\partial t} \end{bmatrix} \begin{Bmatrix} \frac{\partial w}{\partial x} \\ \frac{\partial w}{\partial y} \end{Bmatrix} = [J4] \begin{Bmatrix} \frac{\partial w}{\partial x} \\ \frac{\partial w}{\partial y} \end{Bmatrix} \quad (13)$$

Differentiating Eq. (13) with respect to s and t

$$\begin{Bmatrix} \frac{\partial^2 w}{\partial s^2} \\ \frac{\partial^2 w}{\partial t^2} \\ \frac{\partial^2 w}{\partial s \partial t} \end{Bmatrix} = \begin{bmatrix} \frac{\partial^2 x}{\partial s^2} & \frac{\partial^2 y}{\partial s^2} \\ \frac{\partial^2 x}{\partial t^2} & \frac{\partial^2 y}{\partial t^2} \\ \frac{\partial^2 x}{\partial s \partial t} & \frac{\partial^2 y}{\partial s \partial t} \end{bmatrix} \begin{Bmatrix} \frac{\partial w}{\partial x} \\ \frac{\partial w}{\partial y} \end{Bmatrix} + \begin{bmatrix} -\left(\frac{\partial x}{\partial s}\right)^2 & -\left(\frac{\partial y}{\partial s}\right)^2 & \left(\frac{\partial x}{\partial s} \frac{\partial y}{\partial s}\right) \\ -\left(\frac{\partial x}{\partial t}\right)^2 & -\left(\frac{\partial y}{\partial t}\right)^2 & \left(\frac{\partial x}{\partial t} \frac{\partial y}{\partial t}\right) \\ -\left(\frac{\partial x}{\partial s} \frac{\partial x}{\partial t}\right) & -\left(\frac{\partial y}{\partial s} \frac{\partial y}{\partial t}\right) & \frac{1}{2} \left(\frac{\partial x}{\partial s} \frac{\partial y}{\partial t} + \frac{\partial x}{\partial t} \frac{\partial y}{\partial s}\right) \end{bmatrix} \begin{Bmatrix} \frac{\partial^2 w}{\partial x^2} \\ \frac{\partial^2 w}{\partial y^2} \\ 2\frac{\partial^2 w}{\partial x \partial y} \end{Bmatrix} = [J5] \begin{Bmatrix} \frac{\partial w}{\partial x} \\ \frac{\partial w}{\partial y} \end{Bmatrix} + [J6] \begin{Bmatrix} \frac{\partial^2 w}{\partial x^2} \\ \frac{\partial^2 w}{\partial y^2} \\ 2\frac{\partial^2 w}{\partial x \partial y} \end{Bmatrix} \quad (14)$$

Therefore,

$$\begin{Bmatrix} \frac{\partial^2 w}{\partial x^2} \\ \frac{\partial^2 w}{\partial y^2} \\ 2\frac{\partial^2 w}{\partial x \partial y} \end{Bmatrix} = [J6]^{-1} \begin{Bmatrix} \frac{\partial^2 w}{\partial s^2} \\ \frac{\partial^2 w}{\partial t^2} \\ \frac{\partial^2 w}{\partial s \partial t} \end{Bmatrix} - [J6]^{-1}[J5] \begin{Bmatrix} \frac{\partial w}{\partial x} \\ \frac{\partial w}{\partial y} \end{Bmatrix} \quad (15)$$

From Eq. (13), we have

$$\begin{Bmatrix} \frac{\partial^2 w}{\partial x^2} \\ \frac{\partial^2 w}{\partial y^2} \\ 2\frac{\partial^2 w}{\partial x \partial y} \end{Bmatrix} = [J6]^{-1} \begin{Bmatrix} \frac{\partial^2 w}{\partial s^2} \\ \frac{\partial^2 w}{\partial t^2} \\ \frac{\partial^2 w}{\partial s \partial t} \end{Bmatrix} - [J6]^{-1}[J5][J4]^{-1} \begin{Bmatrix} \frac{\partial w}{\partial s} \\ \frac{\partial w}{\partial t} \end{Bmatrix} \quad (16)$$

Again from Eq. (12),

$$\begin{Bmatrix} \frac{\partial^2 w}{\partial s^2} \\ \frac{\partial^2 w}{\partial t^2} \\ \frac{\partial^2 w}{\partial s \partial t} \end{Bmatrix} = [J3]^{-1} \begin{Bmatrix} \frac{\partial^2 w}{\partial \xi^2} \\ \frac{\partial^2 w}{\partial \eta^2} \\ \frac{\partial^2 w}{\partial \xi \partial \eta} \end{Bmatrix} - [J3]^{-1}[J2][J1]^{-1} \begin{Bmatrix} \frac{\partial w}{\partial s} \\ \frac{\partial w}{\partial t} \end{Bmatrix} \quad (17)$$

Hence Eq. (16) becomes

$$\begin{Bmatrix} -\frac{\partial^2 w}{\partial x^2} \\ -\frac{\partial^2 w}{\partial y^2} \\ 2\frac{\partial^2 w}{\partial x \partial y} \end{Bmatrix} = [J6]^{-1}[J3]^{-1} \begin{Bmatrix} \frac{\partial^2 w}{\partial \xi^2} \\ \frac{\partial^2 w}{\partial \eta^2} \\ \frac{\partial^2 w}{\partial \xi \partial \eta} \end{Bmatrix} - \left([J6]^{-1}[J3]^{-1}[J2][J1]^{-1} + [J6]^{-1}[J5][J4]^{-1}[J1]^{-1} \right) \begin{Bmatrix} \frac{\partial w}{\partial \xi} \\ \frac{\partial w}{\partial \eta} \end{Bmatrix}, \tag{18}$$

where

$$[J1] = \begin{bmatrix} \frac{\partial s}{\partial \xi} & \frac{\partial t}{\partial \xi} \\ \frac{\partial s}{\partial \eta} & \frac{\partial t}{\partial \eta} \end{bmatrix}, \quad [J2] = \begin{bmatrix} \frac{\partial^2 s}{\partial \xi^2} & \frac{\partial^2 t}{\partial \xi^2} \\ \frac{\partial^2 s}{\partial \eta^2} & \frac{\partial^2 t}{\partial \eta^2} \\ \frac{\partial^2 s}{\partial \xi \partial \eta} & \frac{\partial^2 t}{\partial \xi \partial \eta} \end{bmatrix},$$

$$[J3] = \begin{bmatrix} \left(\frac{\partial s}{\partial \xi}\right)^2 & \left(\frac{\partial t}{\partial \xi}\right)^2 & \left(2\frac{\partial s}{\partial \xi} \frac{\partial t}{\partial \xi}\right) \\ \left(\frac{\partial s}{\partial \eta}\right)^2 & \left(\frac{\partial t}{\partial \eta}\right)^2 & \left(2\frac{\partial s}{\partial \eta} \frac{\partial t}{\partial \eta}\right) \\ \left(\frac{\partial s}{\partial \xi} \frac{\partial s}{\partial \eta}\right) & \left(\frac{\partial t}{\partial \xi} \frac{\partial t}{\partial \eta}\right) & \left(\frac{\partial s}{\partial \xi} \frac{\partial t}{\partial \eta} + \frac{\partial s}{\partial \eta} \frac{\partial t}{\partial \xi}\right) \end{bmatrix},$$

$$[J4] = \begin{bmatrix} \frac{\partial x}{\partial \xi} & \frac{\partial y}{\partial \xi} \\ \frac{\partial x}{\partial \eta} & \frac{\partial y}{\partial \eta} \end{bmatrix},$$

$$[J5] = \begin{bmatrix} \frac{\partial^2 x}{\partial s^2} & \frac{\partial^2 y}{\partial s^2} \\ \frac{\partial^2 x}{\partial t^2} & \frac{\partial^2 y}{\partial t^2} \\ \frac{\partial^2 x}{\partial s \partial t} & \frac{\partial^2 y}{\partial s \partial t} \end{bmatrix},$$

$$[J6] = \begin{bmatrix} -\left(\frac{\partial x}{\partial s}\right)^2 & -\left(\frac{\partial y}{\partial s}\right)^2 & \left(\frac{\partial x}{\partial s} \frac{\partial y}{\partial s}\right) \\ -\left(\frac{\partial x}{\partial t}\right)^2 & -\left(\frac{\partial y}{\partial t}\right)^2 & \left(\frac{\partial x}{\partial t} \frac{\partial y}{\partial t}\right) \\ -\left(\frac{\partial x}{\partial s} \frac{\partial x}{\partial t}\right) & -\left(\frac{\partial y}{\partial s} \frac{\partial y}{\partial t}\right) & \frac{1}{2} \left(\frac{\partial x}{\partial s} \frac{\partial y}{\partial t} + \frac{\partial x}{\partial t} \frac{\partial y}{\partial s}\right) \end{bmatrix}.$$

From Eq. (6) all the elements of the matrix [J2] are zeros. Hence Eq. (18) becomes

$$\begin{Bmatrix} -\frac{\partial^2 w}{\partial x^2} \\ -\frac{\partial^2 w}{\partial y^2} \\ 2\frac{\partial^2 w}{\partial x \partial y} \end{Bmatrix} = [[T_{F_1}] \quad [T_{F_2}]] \begin{Bmatrix} \frac{\partial w}{\partial \xi} \\ \frac{\partial w}{\partial \eta} \\ \frac{\partial^2 w}{\partial \xi^2} \\ \frac{\partial^2 w}{\partial \eta^2} \\ \frac{\partial^2 w}{\partial \xi \partial \eta} \end{Bmatrix} \tag{19}$$

or

$$\{\epsilon(x, y)\} = [T] \{\epsilon(\xi, \eta)\}, \tag{20}$$

where $[T_{F_1}] = -[J6]^{-1}[J5][J4]^{-1}[J1]^{-1}$, $[T_{F_2}] = [J6]^{-1}[J3]^{-1}$ and $\{\epsilon(x, y)\}$ and $\{\epsilon(\xi, \eta)\}$ denote the strain vectors in the respective coordinate system. The expression for $\{\epsilon(\xi, \eta)\}$ is given by:

$$\{\epsilon(\xi, \eta)\} = \begin{bmatrix} \frac{\partial w}{\partial \xi} & \frac{\partial w}{\partial \eta} & \frac{\partial^2 w}{\partial \xi^2} & \frac{\partial^2 w}{\partial \eta^2} & \frac{\partial^2 w}{\partial \xi \partial \eta} \end{bmatrix}^T. \tag{21}$$

Using Eq. (8)–(9), Eq. (21) can be rewritten as:

$$\{\epsilon(\xi, \eta)\} = [\bar{B}] \{\delta\}, \tag{22}$$

where $[\bar{B}] = \begin{bmatrix} \frac{\partial N_w}{\partial \xi} & \frac{\partial N_w}{\partial \eta} & \frac{\partial^2 N_w}{\partial \xi^2} & \frac{\partial^2 N_w}{\partial \eta^2} & \frac{\partial^2 N_w}{\partial \xi \partial \eta} \end{bmatrix}^T$.

Hence the combination of Eq. (20)–(22), yields

$$\{\epsilon(x, y)\} = [B] \{\delta\}, \tag{23}$$

where $[B] = [T][\bar{B}]$.

The stress–strain relationship can be expressed as

$$\{\sigma\} = [D] \{\epsilon\} = [D][B] \{\delta\}, \tag{24}$$

where $\{\sigma\}$ is the stress resultant vector given by,

$$\{\sigma\} = [M_x \quad M_y \quad M_{xy}]^T \tag{25}$$

2.6 Stiffness matrix

Total potential energy of the plate element is given by [9]

$$\Pi_p = \frac{1}{2} \iint \{\epsilon(x, y)\}^T \{\sigma(x, y)\} dx dy - \iint w^T dx dy. \tag{26}$$

Applying the principle of minimum potential energy and making appropriate substitutions for $\{\epsilon(x, y)\}$ and $\{\sigma(x, y)\}$, we have

$$[K]_e \{\delta\} = \{P\}_e, \tag{27}$$

where $\{\delta\}$ is the vector of nodal displacements, $\{P\}_e$ is the vector of nodal forces and $[K]_e$ is the plate element stiffness matrix given by

$$[K]_e = \iint [B]^T [D] [B] dx dy. \tag{28}$$

Since the NURBS basis is a function of s and t , Eq. (28) becomes

$$[K]_e = \iint [B]^T [D] [B] |J4| ds dt. \tag{29}$$

Again since $[B]$ is a function of ξ and η , Eq. (29) becomes

$$[K]_e = \iint [B]^T [D] [B] |J1| |J4| d\xi d\eta. \quad (30)$$

The integration is carried out numerically by adopting 2×2 Gaussian quadrature formula.

2.7 Geometric stiffness matrix

The geometric stiffness matrix is formulated considering the action of the in-plane loads causing the bending strains. The membrane strains associated with the small rotations $\frac{\partial w}{\partial x}$ and $\frac{\partial w}{\partial y}$ of the plate mid-surface are given by

$$\{\epsilon_G\} = \begin{Bmatrix} \epsilon_x \\ \epsilon_y \\ \gamma_{xy} \end{Bmatrix} = \begin{Bmatrix} \frac{1}{2} \left(\frac{\partial w}{\partial x} \right)^2 \\ \frac{1}{2} \left(\frac{\partial w}{\partial y} \right)^2 \\ \left(\frac{\partial w}{\partial x} \right) \left(\frac{\partial w}{\partial y} \right) \end{Bmatrix}. \quad (31)$$

The stresses σ_x , σ_y and τ_{xy} are assumed to remain constant, the work done is given by

$$W = \iiint \{\epsilon_G\}^T \{\sigma\} dx dy dz, \quad (32)$$

where

$$\{\sigma\} = [\sigma_x \ \sigma_y \ \tau_{xy}]^T. \quad (33)$$

Now putting the value of $\{\epsilon_G\}$ from Eq. (31) in Eq. (32), we have

$$\begin{aligned} W &= \iiint \left[\frac{1}{2} \left(\frac{\partial w}{\partial x} \right)^2 \ \frac{1}{2} \left(\frac{\partial w}{\partial y} \right)^2 \ \left(\frac{\partial w}{\partial x} \right) \right] \{\sigma\} dx dy dz \\ &= \iiint \frac{1}{2} \{\theta\}^T [\sigma] \{\theta\} dx dy dz, \end{aligned} \quad (34)$$

where

$$\{\theta\} = \left[\frac{\partial w}{\partial x} \ \frac{\partial w}{\partial y} \right]^T \quad (35)$$

and

$$[\sigma] = \begin{bmatrix} \sigma_x & \tau_{xy} \\ \tau_{xy} & \sigma_y \end{bmatrix}. \quad (36)$$

From Eqs. (13) and (11), Eq. (35) can be expressed in terms of ξ and η as

$$\begin{aligned} \{\theta\} &= \begin{Bmatrix} \frac{\partial w}{\partial x} \\ \frac{\partial w}{\partial y} \end{Bmatrix} = [J4]^{-1} \begin{Bmatrix} \frac{\partial w}{\partial s} \\ \frac{\partial w}{\partial t} \end{Bmatrix} \\ &= [J4]^{-1} [J1]^{-1} \begin{Bmatrix} \frac{\partial w}{\partial \xi} \\ \frac{\partial w}{\partial \eta} \end{Bmatrix} = [T_G] \begin{Bmatrix} \frac{\partial w}{\partial \xi} \\ \frac{\partial w}{\partial \eta} \end{Bmatrix}, \end{aligned} \quad (37)$$

where

$$[T_G] = [J4]^{-1} [J1]^{-1} \quad (38)$$

and

$$\begin{Bmatrix} \frac{\partial w}{\partial \xi} \\ \frac{\partial w}{\partial \eta} \end{Bmatrix} = [\bar{B}_G] \{\delta\}, \quad (39)$$

where

$$[\bar{B}_G] = \left[\left[\frac{\partial N_w}{\partial \xi} \ \frac{\partial N_w}{\partial \eta} \right] \right]^T. \quad (40)$$

Combining Eq. (37) and Eq. (39), $\{\theta\}$ can be expressed as

$$\{\theta\} = [T_G] [\bar{B}_G] \{\delta\} = [B_G] \{\delta\}, \quad (41)$$

where

$$[B_G] = [T_G] [\bar{B}_G]. \quad (42)$$

Now substituting the value of $\{\theta\}$ from Eq. (41), Eq. (34) becomes

$$\begin{aligned} W &= \iiint \frac{1}{2} \{\delta\}^T [B_G]^T [\sigma] [B_G] \{\delta\} dx dy dz \\ &= \frac{t}{2} \iint \{\delta\}^T [B_G]^T [\sigma] [B_G] \{\delta\} dx dy dz. \end{aligned} \quad (43)$$

The external work done by the nodal force is given by

$$W = \frac{1}{2} \{\delta\}^T [K_G] \{\delta\}. \quad (44)$$

From Eqs. (43) and (44), the geometric stiffness matrix of the plate element can be written as

$$\begin{aligned} [K_G] &= t \iint [B_G]^T [\sigma] [B_G] dx dy \\ &= t \iint [B_G]^T [\sigma] [B_G] |J4| ds dt \\ &= t \iint [B_G]^T [\sigma] [B_G] |J1| |J4| d\xi d\eta. \end{aligned} \quad (45)$$

2.8 Boundary conditions

Reproducing the procedures adopted in [1, 9], as a general case, the stiffness matrix for a curved boundary supported on elastic springs continuously spreads in the directions of all possible displacements and rotations along the boundary line is formulated from which the specific boundary conditions can be obtained by incorporating the appropriate value of spring constants. Considering a local axis system $x_1 - y_1$ at a point P on a curved boundary along the direction of the normal to the boundary at that point as shown in Fig. 3, the displacement components along it can be found. Let β be the angle made by the local axis $x_1 - y_1$ with the global axis $x - y$.

Hence the relationship between the two axes is given by

$$\begin{Bmatrix} x \\ y \end{Bmatrix} = \begin{bmatrix} \cos \beta & -\sin \beta \\ \sin \beta & \cos \beta \end{bmatrix} \begin{Bmatrix} x_1 \\ y_1 \end{Bmatrix}. \tag{46}$$

The displacements at P which may be restrained can be expressed as

$$\{f_b\} = \begin{Bmatrix} w \\ \theta_n \\ \theta_t \end{Bmatrix} = \begin{Bmatrix} w \\ \frac{\partial w}{\partial x_1} \\ \frac{\partial w}{\partial y_1} \end{Bmatrix}, \tag{47}$$

where θ_n and θ_t represent the slopes which are normal and transverse to the boundaries, respectively. Substituting from Eq. (46), Eq. (47) can be written as

$$\{f_b\} = \begin{bmatrix} 1 & 0 & 0 \\ 0 & \cos \beta & \sin \beta \\ 0 & -\sin \beta & \cos \beta \end{bmatrix} \begin{Bmatrix} w \\ \frac{\partial w}{\partial x} \\ \frac{\partial w}{\partial y} \end{Bmatrix}. \tag{48}$$

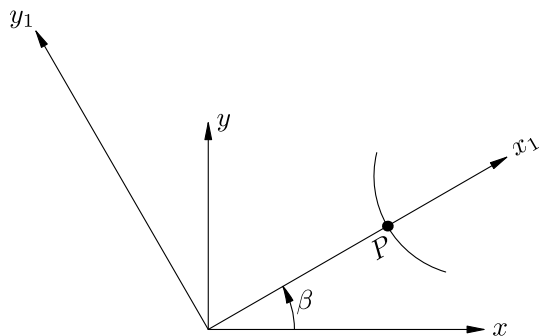


Fig. 3 Coordinate axes at any point of an elastically restrained curved boundary

Expressing Eq. (48) in terms of the shape functions, we have

$$\{f_b\} = [N_b]\{\delta\}, \tag{49}$$

$$[N_b] = \begin{bmatrix} 1 & 0 & 0 \\ 0 & \cos \beta & \sin \beta \\ 0 & -\sin \beta & \cos \beta \end{bmatrix} \begin{Bmatrix} [N_w] \\ \frac{\partial [N_w]}{\partial x} \\ \frac{\partial [N_w]}{\partial y} \end{Bmatrix}. \tag{50}$$

Let $k_w, k_\alpha,$ and k_β be the spring constants or restraint coefficients corresponding to the direction of w, θ_n and $\theta_t,$ respectively. The reaction components per unit length along the boundary line due to the spring constants corresponding to the possible boundary displacements are given by

$$\{f_k\} = \begin{Bmatrix} f_{kw} \\ f_{k\alpha} \\ f_{k\beta} \end{Bmatrix} = \begin{Bmatrix} k_w w \\ k_\alpha \theta_n \\ k_\beta \theta_t \end{Bmatrix}. \tag{51}$$

Equation (51) can be rewritten by combining Eqs. (47)–(49) as

$$\{f_k\} = [N_k]\{\delta\}, \tag{52}$$

$$\text{where } [N_k] = \begin{bmatrix} k_w & 0 & 0 \\ 0 & k_\alpha \cos \beta & k_\alpha \sin \beta \\ 0 & -k_\beta \sin \beta & k_\beta \cos \beta \end{bmatrix} \begin{Bmatrix} [N_w] \\ \frac{\partial [N_w]}{\partial x} \\ \frac{\partial [N_w]}{\partial y} \end{Bmatrix}.$$

Using Eqs. (48) and (51), the stiffness matrix can be obtained by the virtual work principle and is expressed as

$$[K_b] = \int [N_b]^T [N_k] |J_b| d\lambda_1, \tag{53}$$

where λ_1 is the direction of the boundary line in the $\xi - \eta$ plane and Jacobian $|J_b| = \frac{ds_1}{d\lambda_1}$. The value of the Jacobian

along a boundary line is considered as a ratio of the actual length to the length on the mapped domain considering any segment of the boundary line. A classical boundary condition can be attained by substituting a high value of the restraint coefficients corresponding to the restraint direction.

3 Numerical examples

The stability analyses of a number of plates having different shapes and boundary conditions are carried out using the simultaneous iteration algorithm of Corr and

Jennings [5] and the results obtained are compared with the existing ones. The results are presented in tabular form with a mesh division of 32×32 for the whole plate. Figures of typical plates showing mesh divisions of 8×8 along with the nodes (asterisk) are presented for each case. The abbreviations used in the table for the boundary conditions (S—simply supported, C—clamped, F—free) are depicted in the anti-clockwise direction starting from the left edge of the plate. The ability of NAFEM to analyse some new shapes is showcased by considering a rectangular plate with one side curved edge consisting of a rectangular portion as patch-1 and the remaining as patch-2.

3.1 Circular plate

The buckling loads for the simply supported and the clamped bare circular plates are computed and the results are presented in the form of the parameter $k = (N_r)_{cr} a^2 / D$, where $(N_r)_{cr}$ is the critical compressive force uniformly around the edge of the plate, a is the radius of the circular plate and D is the flexural rigidity of the plate. The results are presented in Table 1 for various mesh divisions of the whole plate to study the convergence of the buckling parameter and they are compared with the analytical values of Timoshenko and Gere [19]. There is excellent agreement between the results (Fig. 4).

3.2 Rectangular plate with curved edges

A rectangular plate having curved edges (Fig. 5) is analysed for different boundary conditions and aspect ratios r_1/r_2 (where r_1 and r_2 are the semi-major and semi-minor

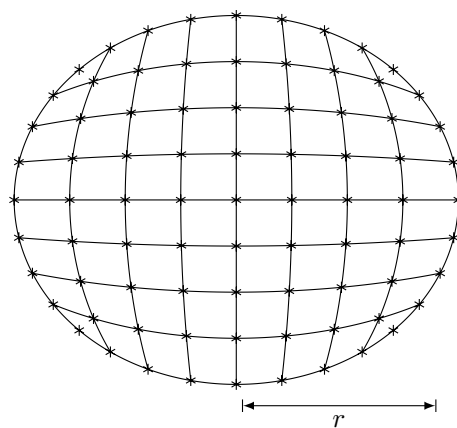


Fig. 4 A typical circular plate having 8×8 mesh

axes of the plate, respectively) that are presented in Tables 2 and 3.

3.3 Semi-circular semi-elliptical plate

The stability analysis of a plate consisting of a semi-circle and semi-ellipse (Fig. 6) is carried out for different boundary conditions and aspect ratios a/b (where a is the radius of the semi-circle and the semi-minor axis of the semi-ellipse and b is the semi-major axis of the semi-ellipse) and the results are presented in Tables 4 and 5.

3.4 Dome-shaped plate

A typical plate resembling the shape of a dome is considered by taking one of the edges straight and its opposite edge as the top of a dome (Fig. 7). The stability analysis

Table 1 Buckling parameter $k = (N_r)_{cr} a^2 / D$ for uniformly compressed clamped and simply supported circular plates ($\nu = 0.3$)

Boundary condition	Mesh size	Present analysis	Timoshenko and Gere [19]
Clamped	2×2	18.048	14.68
	4×4	15.959	
	8×8	14.777	
	16×16	14.685	
	32×32	14.681	
Simply supported	2×2	3.1476	4.20
	4×4	3.8908	
	8×8	4.1144	
	16×16	4.1764	
	32×32	4.1924	

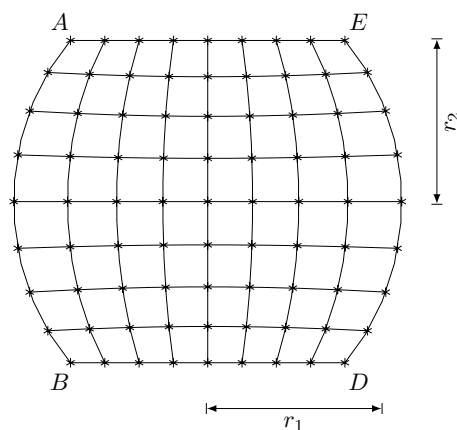


Fig. 5 A typical rectangular plate with curved edges having 8×8 mesh

Table 2 Buckling load parameter $k = \lambda r_1^2 / \pi^2 D$ for biaxially compressed rectangular plate with curved edges

Support condition	Aspect ratio r_1/r_2						
	1.0	1.5	2.0	2.5	3.0	3.5	4.0
SSSS	0.71166	1.3347	2.236	3.4056	4.808	6.4742	8.388
CCCC	2.1254	4.4427	7.9233	12.432	17.938	24.436	31.925
CCSS	1.2372	2.4378	4.199	6.4898	9.2932	12.599	16.396
CSCS	1.2015	1.7273	2.5617	3.6702	5.0398	6.6662	8.5476
SCSC	1.7793	4.0339	6.6394	9.5241	12.775	16.411	20.291
CFCF	1.2085	1.0758	1.0026	0.96181	0.93556	0.92375	0.91465
FCFC	0.90863	1.5608	2.1185	2.5834	2.9723	3.3179	3.6372
FSFS	0.52899	1.1545	1.6692	2.0923	2.4457	2.7372	2.9939
SFSF	0.45808	0.7837	0.92723	0.90515	0.89072	0.885	0.87878
FFCC	0.22887	0.36918	0.55356	0.78208	1.0384	1.3093	1.5774
FFSS	0.11392	0.14488	0.15506	0.15762	0.15763	0.15693	0.15611

Table 3 Buckling load parameter $k = \lambda r_1^2 / \pi^2 D$ for uniaxially compressed rectangular plate with curved edges

Support condition	Aspect ratio r_1/r_2						
	1.0	1.5	2.0	2.5	3.0	3.5	4.0
SSSS	2.0404	5.1509	8.1281	13.157	21.194	25.941	33.1247
CCCC	4.8887	8.8438	15.314	23.273	32.127	43.688	56.115
CCSS	2.8711	6.077	10.792	1.262	24.731	33.619	44.55
CSCS	2.8146	5.978	9.2513	13.906	19.449	26.499	34.29
SCSC	3.2760	7.1407	13.025	19.5	28.458	39.295	51.045
CFCF	1.4092	1.5068	1.5738	1.6246	1.6673	1.7065	1.7443
FCFC	1.0568	1.7401	2.2794	2.7128	3.08	3.4066	3.7098
FSFS	0.80973	1.3733	1.8742	2.2661	2.5824	2.8474	3.0781
SFSF	0.5541	0.91456	1.212	1.3862	1.4933	1.5694	1.6219
FFCC	0.4244	0.81065	1.2015	1.5892	1.9472	2.2824	2.5875
FFSS	0.23789	0.4715	0.74787	1.0518	1.3551	1.6372	1.895

Table 4 Buckling load parameter $k = \lambda b^2 / \pi^2 D$ for biaxially compressed semi-circular semi-elliptical plate

Support condition	Aspect ratio a/b						
	1.125	1.25	1.5	1.75	2.0	2.25	2.5
SSSS	0.50947	0.6015	0.81242	1.0606	1.3459	1.6672	2.0231
CCCC	1.7872	2.1072	2.8178	3.6551	4.6128	5.6917	6.8922
CCSS	1.0083	1.1933	1.6172	2.1154	2.6873	3.3298	4.0394
CSCS	1.2025	1.343	1.6286	1.9176	2.2331	2.5711	2.9342
CFCF	1.0202	1.2142	1.4591	1.646	1.811	1.9436	2.0592
FCFC	1.0264	1.2163	1.6019	1.9696	2.3132	2.369	2.9499
FSFS	0.5688	0.5988	0.80066	1.0327	1.289	1.5776	1.8828
SFSF	0.50964	0.60172	0.80721	1.0459	1.3187	1.6348	1.8199
FFCC	0.23163	0.27243	0.35959	0.45335	0.55311	0.65858	0.76969
FFSS	0.17966	0.21288	0.28	0.34573	0.40832	0.46674	0.52051

of this dome-shaped plate is carried out for different boundary conditions and aspect ratio r_1/r_2 , where r_1 is the length of the straight edge and r_2 is the semi-minor axis of the dome. The results obtained are presented in Tables 6 and 7.

3.5 Rectangular plate with one side curved edge

A rectangular plate with one side being curved is analysed by considering the rectangular portion as patch-1 (32×32 mesh) and the remaining portion as patch-2 (32×32 mesh) subjected to uniaxial and biaxial compression

Table 5 Buckling load parameter $k = \lambda b^2 / \pi^2 D$ for uni-axially compressed semi-circular semi-elliptical plate

Support condition	Aspect ratio a/b						
	1.125	1.25	1.5	1.75	2.0	2.25	2.5
SSSS	1.0793	1.3533	2.0464	2.9428	3.9984	5.1705	6.4633
CCCC	3.4418	4.1802	5.8939	7.7924	9.9082	12.239	14.795
CCSS	2.1096	2.6738	4.0967	5.8054	7.3749	9.0295	11.009
CSCS	2.1078	2.4683	3.2852	4.2262	5.345	6.6454	8.1413
SCSC	2.9397	3.5355	4.9687	6.7713	8.9825	11.371	13.666
CFCF	1.5358	1.7116	2.0449	2.3539	2.6393	2.9029	3.1471
FCFC	1.1938	1.4061	1.8264	2.1826	2.5298	2.8451	3.1457
FSFS	0.79463	0.9488	1.2881	1.6222	1.9344	2.2068	2.4468
SFSF	0.77122	0.90106	1.1764	1.4481	1.703	1.9359	2.1472
FFCC	0.44179	0.54292	0.78461	1.0758	1.4062	1.7846	2.1849
FFSS	0.36032	0.44731	0.64655	0.87978	1.1416	1.4434	1.7906

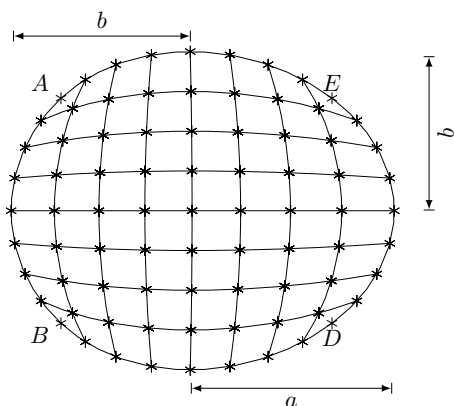


Fig. 6 A typical semi-circular semi-elliptical plate having 8×8 mesh

under different boundary conditions and aspect ratios (a —half of the length of the rectangular portion; b —breadth of the rectangular portion). The nodes of the rectangular portion (patch-1) are represented with asterisk

and the remaining portion (patch-2) with circular markers, respectively. The results obtained are presented in Tables 8 and 9. A typical rectangular plate with one side curved consisting of a rectangular portion as patch-1 (4×4 mesh) and the remaining as patch-2 (4×4 mesh) is shown in Fig. 8.

4 Conclusions

In the present formulation, NURBS basis functions are used to represent the exact shape of the arbitrary thin plates. In contrast to the isogeometric analysis, the use of classical finite element basis functions as field variables helps in imposing the boundary conditions easily which is the main drawback of isogeometric analysis. Further, the knot refinement technique of the NURBS basis function takes care of the mesh generation. The stability analyses of the arbitrary shaped plates are carried out and the results obtained are found to be well in

Table 6 Buckling load parameter $k = \lambda r_1^2 / \pi^2 D$ for uni-axially compressed dome-shaped plate

Support condition	Aspect ratio r_1/r_2						
	1.0	1.5	2.0	2.5	3.0	3.5	4.0
SSSS	0.92116	2.6223	4.9068	7.3203	10.42	13.87	17.767
CCCC	2.6381	5.3275	8.5076	12.715	17.777	23.506	30.016
CCSS	1.5718	3.9923	6.6373	9.8915	13.819	18.471	23.708
CSCS	1.6826	2.9994	5.1835	7.8613	10.656	14.02	18.119
SCSC	2.4942	4.5597	7.9851	12.628	17.317	23.243	30.022
CFCF	0.99238	1.0785	1.1642	1.2466	1.3241	1.3961	1.4626
FCFC	0.866991	1.7341	2.6787	3.7163	4.8407	6.0745	7.3658
FSFS	0.62767	1.176	1.8784	2.5593	3.2623	3.994	4.7453
SFSF	0.32856	0.4714	0.66202	0.84867	1.0031	1.1226	1.2175
FFCC	0.24119	0.44356	0.63387	0.82257	1.004	1.1749	1.3362
FFSS	0.20103	0.38655	0.5021	0.62451	0.74336	0.86184	0.97197

Table 7 Buckling load parameter $k = \lambda r_1^2 / \pi^2 D$ for biaxially compressed dome-shaped plate

Support condition	Aspect ratio r_1/r_2						
	1.0	1.5	2.0	2.5	3.0	3.5	4.0
SSSS	0.43082	0.74445	1.2152	1.8212	2.5658	3.4405	4.4442
CCCC	1.3453	2.4319	4.1078	6.3153	9.0261	12.299	15.997
CCSS	0.79178	1.3765	2.2768	3.4623	4.8976	6.6143	8.6006
CSCS	0.91935	1.1326	1.5221	2.0705	2.7639	3.5954	4.5619

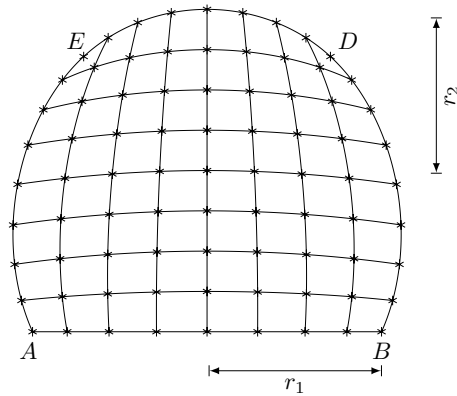


Fig. 7 A typical dome-shaped plate having 8×8 mesh

agreement in all the cases. To showcase the robustness of NAFEM some plates of different geometries (semi-circular semi-elliptical, rectangular plate with curved edges and dome-shaped plate) have been considered for the stability analysis and the new results are presented. Further a rectangular plate with one side being curved is analysed by considering the rectangular portion as patch-1 and the remaining portion as patch-2, thereby showing the capability of NAFEM to analyse certain geometries by breaking them into more amenable patches which can be dealt with ease.

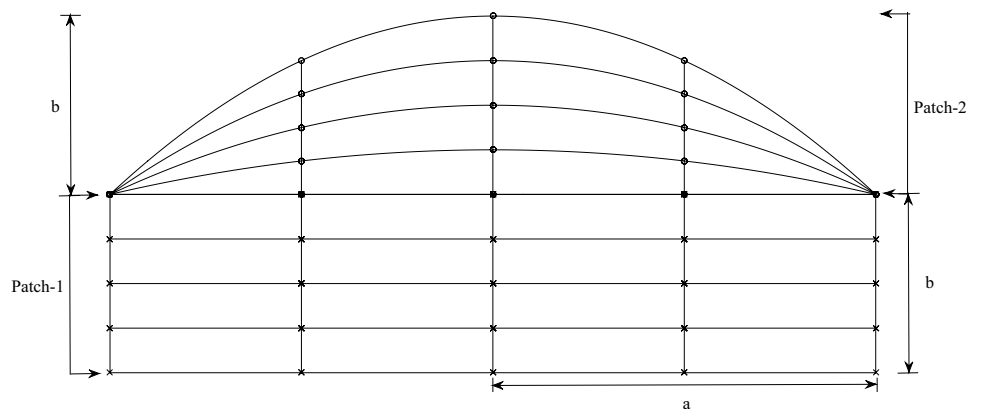
Table 8 Buckling load parameter $k = \lambda a^2 / \pi^2 D$ for biaxially compressed rectangular plate with one side curved edge

Support condition	Aspect ratio r_1/r_2						
	1.15	1.35	1.55	1.75	2.15	2.35	2.55
CCCC	1.7989	2.2276	2.7417	3.352	4.8227	5.6894	6.6165
SSSS	0.5585	0.6745	0.8151	0.9801	1.3807	1.6153	1.8723
CCSS	0.9191	1.1564	1.4476	1.7908	2.6184	3.1039	3.6351

Table 9 Buckling load parameter $k = \lambda a^2 / \pi^2 D$ for uniaxial compressed rectangular plate with one side curved edge

Support condition	Aspect ratio r_1/r_2						
	1.15	1.35	1.55	1.75	2.15	2.35	2.55
CCCC	3.5888	4.7096	5.9017	7.1686	10.022	11.658	13.43
SSSS	1.2715	1.8413	2.6341	3.6633	5.62	6.5834	7.6277
CCSS	2.0263	2.9892	4.1526	5.2174	7.548	8.8727	10.328

Fig. 8 A typical rectangular plate with one side curved edge consisting of a rectangular portion as patch-1 (4×4 mesh) and the remaining as patch-2 (4×4 mesh)



References

- Barik M, Mukhopadhyay M (1998) Finite element free flexural vibration analysis of arbitrary plates. *Finite Elem Anal Des* 29:137–151
- Barik M, Mukhopadhyay M (2002) A new stiffened plate element for the analysis of arbitrary plates. *Thin-Walled Struct* 40:625–639
- da Veiga Beirão L, Buffa A, Lovadina C, Martinelli M, Sangalli G (2012) An isogeometric method for the Reissner-Mindlin plate bending problem. *Comput Methods Appl Mech Eng* 209–212:45–53
- Belytschko T, Lu Y, Gu L (1994) Element free Galerkin methods. *Int J Numer Meth Engng* 37:229–256
- Corr RB, Jennings E (1976) A simultaneous iteration algorithm for solution of symmetric eigen value problem. *Int J Numer Meth Eng* 10:647–663
- Embar A, Dolbow J, Harari I (2010) Imposing Dirichlet boundary conditions with Nitsche's method and spline based finite elements. *Int J Numer Meth Engng* 83:877–898
- Hughes TJR, Cottrell JA, Bazilevs Y (2005) Isogeometric analysis: CAD, finite elements, NURBS, exact geometry and mesh refinement. *Comput Methods Appl Mech Eng* 194:4135–4195
- Liew KM, Xiang Y, Kitipornchai S (1996) Analytical buckling solutions for mindlin plates involving free edges. *Int J Mech Sci* 10(38):1127–1138
- Mishra BP, Barik M (2017) NURBS-augmented finite element method for static analysis of arbitrary plates. *Comput Struct*. <https://doi.org/10.1016/j.compstruc.2017.10.011>
- Mitchell TJ, Govindjee S, Taylor RL (2011) A method for enforcement of dirichlet boundary conditions in isogeometric analysis. In: Mueller-Hoeppe D, Loehnert S, Reese S (eds) *Recent developments and innovative applications in computational mechanics*. Springer, Berlin, pp 283–293
- Nguyen VP, Anitescu C, Bordas SPA, Rabczuk T (2015) Isogeometric analysis: An overview and computer implementation aspects. *Math Comput Simul* 117:89–116
- Sevilla R, Fernández S, Huerta A (2008) NURBS-enhanced finite element method (NEFEM). *Int J Numer Meth Engng* 76:56–83
- Shojaee S, Izadpanah E, Valizadeh N, Kiendl J (2012) Free vibration analysis of thin plates by using a NURBS-based Isogeometric approach. *Finite Elem Anal Des* 61:23–34
- Shojaee S, Valizadeh N, Izadpanah E, Bui T, Vu TV (2012) Free vibration and buckling analysis of laminated composite plates using the NURBS-based Isogeometric finite element method. *Compos Struct* 94:1677–1693
- Thai CH, Ferreira AJM, Bordas SPA, Rabczuk T, Nguyen-Xuan H (2014) Isogeometric analysis of laminated composite and sandwich plates using a new inverse trigonometric shear deformation theory. *Eur J Mech A Solids* 43:89–108
- Thai CH, Ferreira AJM, Carrera E, Nguyen-Xuan H (2013) Isogeometric analysis of laminated composite and sandwich plates using a layerwise deformation theory. *Compos Struct* 104:196–214
- Thai CH, Nguyen-Xuan H, Bordas SPA, Nguyen-Thanh N, Rabczuk T (2015) Isogeometric analysis of laminated composite plates using the higher-order shear deformation theory. *Mech Adv Mater Struct* 22(6):451–469
- Thai CH, Nguyen-Xuan H, Nguyen-Thanh N, Le TH, Nguyen-Thoi T, Rabczuk T (2012) Static, free vibration, and buckling analysis of laminated composite ReissnerMindlin plates using NURBS-based isogeometric approach. *Int J Numer Methods Eng* 91(6):571–603
- Timoshenko SP, Gere JM (1963) *Theory of elastic stability*, 2nd edn. McGraw-Hill International, New York
- Valizadeh N, Natrajan S, Gonzalez-Estrada OA, Rabczuk T, Bui TQ, Bordas SPA (2013) NURBS-based finite element analysis of functionally graded plates: Static bending, vibration, buckling and flutter. *Compos Struct* 99:309–326
- Wang X, Zhu X, Hu P (2015) Isogeometric finite element method for buckling analysis of generally laminated composite beams with different boundary conditions. *Int J Mech Sci* 104:190–199
- Woinowsky-Krieger S (1937) The stability of a clamped elliptic plate under uniform compression. *J Appl Mech* 4(4):177–178
- Zhou Y, Zheng X, Harik IE (1995) Buckling of triangular plates under uniform compression. *J Appl Mech* 5(57):847–854
- Zhu T, Atluri SN (1998) A modified collocation method and a penalty formulation for enforcing the essential boundary conditions in Element free Galerkin method. *Comp Mech* 21:211–222